European Journal of Radiology 144 (2021) 109995

Contents lists available at ScienceDirect

European Journal of Radiology

journal homepage: www.elsevier.com/locate/ejrad

Four functional magnetic resonance imaging techniques for skeletal muscle exploration, a systematic review

Sergio Caroca [a], Diego Villagran [b], Steren Chabert [a,c,d,*]

[a] Biomedical Engineering Department, Universidad de Valparaiso, Valparaíso, Chile
[b] Servicio de Imagenología, Hospital Carlos van Buren, Valparaíso, Chile
[c] CINGS, Centro de Investigación y Desarrollo en INGeniería en Salud, Universidad de Valparaiso, Valparaíso, Chile
[d] Millennium Nucleus for Cardiovascular Magnetic Resonance, Chile

ARTICLE INFO

Keywords:
Functional MRI
BOLD
ASL
IVIM
DCE
Skeletal muscle

ABSTRACT

Background: The study of muscle health has become more relevant lately, due to global aging and a higher incidence of musculoskeletal pathologies. Current exploration techniques, such as electromyography, do not provide accurate spatial information.

Objective: The objective of this work is to perform a systematic review of the literature to synthesize the contributions that can offer functional MRI techniques commonly used in neuroimaging, applied to skeletal muscle: Blood Oxygen Level Dependent (BOLD), IntraVoxel Incoherent Motion (IVIM), Arterial Spin Labeling (ASL) and Dynamic Contrast Enhanced (DCE).

Evidence acquisition: Web of Science and Medline databases were searched, over the last 10 years, focused on the use of BOLD, ASL, IVIM or DCE in skeletal muscle.

Evidence synthesis: 59 articles were included after applying the selection criteria. 37 studies were performed in healthy subjects, and 22 in patients with different pathologies: in peripheral arterial disease, systemic sclerosis, diabetes, osteoporosis, adolescent idiopathic scoliosis, and dermatomyositis. Reference values in healthy subjects still vary in some cases.

Conclusion: The studies show the feasibility of implementing functional MRI through BOLD, ASL, IVIM or DCE imaging in several muscles and their possible utility in different pathologies. A synthesis of how to implement such exploration is given here.

Clinical impact: These four techniques are based on sequences already present in clinical MRI scanners, therefore, their use for functional muscle exploration does not require additional investment. These techniques allow visualization and quantification of parameters associated with the vascular health of the muscles and represent interesting support for musculoskeletal exploration.

1. Introduction

The study of muscle health involves a set of techniques and procedures whose main purpose is to monitor the composition and functioning of muscles. In recent times, this concept has gained relevance due to the global aging of the population worldwide, which leads to a higher incidence of pathologies related to the musculature [1,2]. Electromyography has been one of the method of interest, for its accessibility and high temporal resolution, but it lacks spatial resolution and imaging ability. Additionally, the structure of the anatomy of muscle, or even its basal perfusion levels, might not be enough to distinguish a healthy tissue from a pathological one [3]. A possible solution to this problem lies in the use of imaging techniques and functional imaging using MRI, which can generate new possibilities for muscle imaging. Four techniques in particular draw attention to functional exploration focused on the observation of blood flow, or observation of the microperfusion of the tissues, or direct observation of the aerobic energy consumption, respectively with sequences of the Arterial Spin Labeling (ASL) type, or IntraVoxel Incoherent Motion (IVIM), or the commonly called functional Magnetic Resonance Imaging (fMRI) based on BOLD (Blood Oxygen Level Dependent) signal, or with Dynamic Contrast-Enhanced (DCE) images, based on the intravenous injection of a contrast media. These are techniques whose principles are not new, especially in the context of functional brain imaging [4–6] but the extension of their

* Corresponding author at: Escuela de Ingenieria Civil Biomedica, General Cruz 222, Valparaiso, Chile.
E-mail address: steren.chabert@uv.cl (S. Chabert).

https://doi.org/10.1016/j.ejrad.2021.109995
Received 25 August 2021; Received in revised form 27 September 2021; Accepted 29 September 2021
Available online 4 October 2021

application outside the brain is gaining increasing interest in the last decade. The question then arises as to what observations have been achieved to date through these three functional MRI techniques in the functional exploration of skeletal muscle. Pathologies such as peripheral arterial disease (PAD), or diabetes, can affect the vasculature density or the vessel diameters, which in turn will impact on the tissue oxygenation and therefore the muscle function. There are also myopathies that can affect muscle type-I vs. type-II fibers differently [3,7]. On another hand, aging is a huge public health problem in modern society, which is associated with reduced microvascular function. It has been suggested that aerobic exercise interventions may improve microvascular function in older adults. To count on exploration techniques that could go beyond the anatomy and explore the muscle function, can be of help to diagnose and monitor the progression of pathology, or of treatment.

BOLD imaging is based on the difference in magnetic susceptibility between oxyhemoglobin (diamagnetic) and deoxyhemoglobin (paramagnetic). The increase of local aerobic energy consumption, and the associated variation of cerebral blood flow, induce a local increase in venous oxyhemoglobin, as the increase in local blood flow is bigger than the oxygen consumption itself. The change in venous oxy- vs. deoxyhemoglobin ratio induces a change in the global magnetic susceptibility. This change in susceptibility is evidenced in an alteration in the transversal relaxation time T2*, affecting the measured signal, thus allowing to generate a contrast between signal “activated” vs signal “at rest”. A review of biophysical model of BOLD signal is available in [8]. Imaging is performed using the conventional gradient-echo echo planar imaging (EPI) sequence for several minutes while the patient is performing the task under study, looking for the contrast between the signal strength during the “task” and during “rest”. It is an indirect measurement of brain activity, widely used not only in cognitive sciences but also in clinical, pre-surgical, or psychiatric applications [9]. Although BOLD is widely used in the brain, the mechanisms underlying oxygen consumption, and thus BOLD signal, are different, as well as the implementation of functional observation itself. Then the question arises of knowing what has been observed so far with fMRI-BOLD in muscle imaging, and how.

On the other hand, the arterial spin labeling (ASL) sequences allow characterization and quantification of tissue perfusion without the need for a contrast agent [6]. Widely used for measuring cerebral blood flow, it consists of magnetic labeling of the hydrogen molecules contained in the water in the arterial blood. This labeling is done by using a radio frequency pulse in an anterior area of the slice of interest according to the direction of blood flow. This labeled blood is considered an endogenous tracer. After a definite period of time, the magnetic tracers flow into the area of interest, and an image is obtained there. The final calculated map is the blood flow map, obtained by subtracting the marked image from the control image. More details about its implementation and clinical interest in the context of neuroradiology are found in Grade et al. 2015 [10].

The third technique of interest here is the one that refers to the measurement of the diffusion of molecules in tissues at low b values, through Intra-Voxel Incoherent Motion (IVIM). The IVIM arose from the observation obtained in multiple tissues that showed a decay of the biexponential type signal in the initial part of the curve, beyond the classic monoexponential model in diffusion, as indicated in equation (1).

$$\frac{S}{S_0} = (1-f)^{*}e^{-bD} + f^{*}e^{-bD^{*}} \quad (1)$$

where b corresponds to the diffusion weighting, S to the diffusion-weighted signal, S_0 to the signal without diffusion weighting, D is the diffusion coefficient observed in tissues, D^* is called pseudo-diffusion coefficient, and f perfusion fraction [4]. The presence of capillaries with an apparently random orientation at the voxel level implies a translational movement of the molecules in these capillaries, which is associated with a rapid diffusion movement, visible at low values of b. Several studies have associated the IVIM parameters, f, and D^*, to the microperfusion present in the tissues, in particular, f has been associated with the blood volume and D^* with the average transit time [11]. The acquisition itself is performed using a DW-MRI sequence with multiple values of b, and the images are processed according to equation (1). Most applications of IVIM to date have been focused on the exploration of microperfusion, in particular in relation to oncology, and some of them in association with BOLD functional imaging with a rest/activity scheme, as reviewed by Le Bihan in [12].

Finally, the last technique corresponds to DCE. The injection of contrast media is used most commonly to visualize the patient vasculature and, using pharmacokinetic modeling, it is possible to quantify the tissue perfusion [13]. This is done by adjusting an arterial input function (AIF), that is convolved with an impulse retention function; the perfusion quantification is then adjusted to fit the measured signal in the voxel time serie. DCE has been commonly used to assess perfusion in general; the present question is if it is possible to go beyond the observation of a steady-state tissue perfusion, and to manage the contrast injection set-up to evaluate perfusion changes related to exercising muscles.

The four techniques correspond to acquisition sequences present in most clinical MRI scanners – gradient-echo EPI, DW-MRI sequence, or ASL. This implies that, by confirming the contribution these images can make to the study of muscle health, studies could be implemented without major difficulty. This paper aims to review the literature to synthesize the contributions that can deliver these three functional MRI scanning techniques, their recent application in skeletal muscle, and summarize the implementation that has been used.

2. Materials and methods

A systematic review of the literature was performed by searching the PubMed and Web of Science databases. The search expression was established by considering the following terms: “Magnetic Resonance Imaging“, “skeletal muscle”, “perfusion“, “BOLD”, “IVIM“, “ASL” or “DCE”, leading to the search expression: “Magnetic Resonance Imaging” and “skeletal muscle“ and (perfusion or BOLD or IVIM or ASL or DCE).

The inclusion criteria defined were: 1) to have been published since 2010 to the date of search; 2) with full text accessible in English; 3) include at least one of the techniques in the procedure; 4) skeletal muscle study and 5) studies in human subjects. The following exclusion criteria were defined: 1) perform the functional exploration of the muscle using exclusively other techniques than those defined here; 2) tumor studies; 3) cardiac muscle studies, 4) functional brain imaging studies associated with motor control, 5) review papers or conference abstracts with brief publication format. Articles focused on the development of new sequences were also excluded.

The search was implemented in the first week of October 2020. The screening and selection of articles were performed independently by two authors of this work (SA and SC). The included papers were then analyzed in common, and agreements were found for the discrepancies that occurred in the first screening analysis.

Different themes were defined to be extracted from each study: first, to observe the way of implementation of each functional examination: to identify the set of observed muscles, proposed muscle activation mechanisms, and acquisition schemes. For each imaging technique, the range of pathologies studied was observed, highlighting the type of observations obtained, the associated interpretation, and the sensitivity of the measurements.

3. Results

As summarized in Fig. 1, the search expression yielded a total of 405 papers, of which 59 were included. Of these, 27 correspond to procedures performed using the BOLD technique, 8 with ASL, 12 with IVIM and 5 with DCE, in addition to 7 studies that combined two or three of the

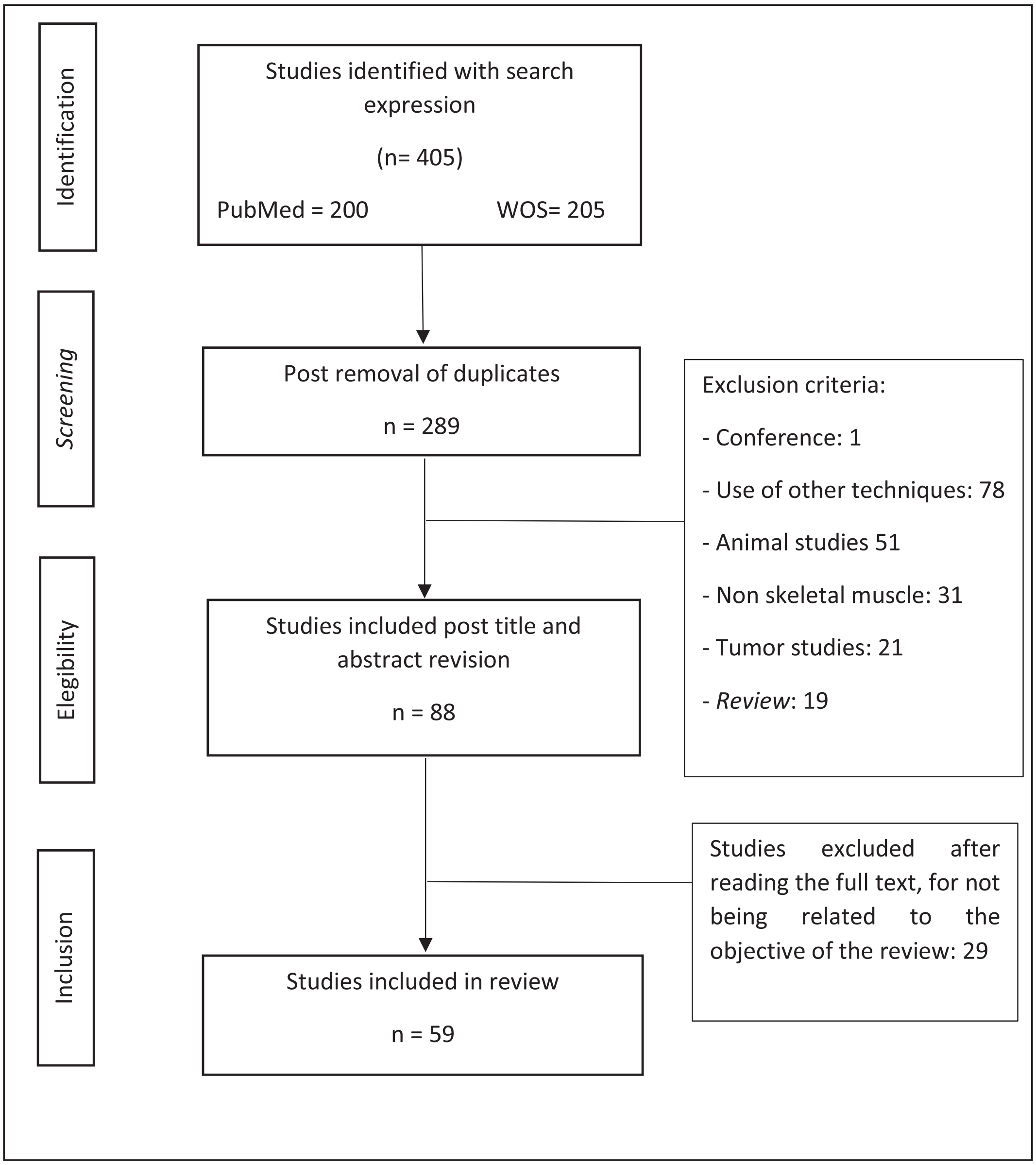

Fig. 1. Flow diagram for the process of paper selection.

techniques studied. Of this total, 37 were performed only in healthy subjects, summarized in Table 1 and 22 in patients with certain pathology, presented in Table 2.

3.1. Implementation of functional studies

For the three techniques studied, the main focus observed is on the study of the lower limbs, particularly the calf, gastrocnemius and soleus muscles [3,14–64]. Several works also show results in lumbar muscles [65–68], arm and shoulder [69–71].

The muscle activation mechanisms were of two types; The first and most used was the "ischemia-hyperemia paradigm"; The second corresponds to muscle activation exercises. In the case of the ischemia-hyperemia paradigm, the inflation and deflation of a cuff are used. The first stage, of insufflation, induces the phenomenon of ischemia. The cuff is then deflated and an abrupt oxygenation stage of reactive hyperemia is observed. The application parameters of this paradigm are the duration and the pressure value. Taking into account the median values, an inflation time of 5 min is used, with an applied pressure of 50 mm Hg in BOLD studies and 110 mm Hg in ASL – different groups have implemented this paradigm in a different way and no standard is set yet. The main advantage of this activation method lies in its greater ability to control stimulation and its easy reproducibility: an intra-class correlation coefficient (ICC) of 0.98 has been reported in ASL studies with this method compared to ICC 0.87 in the case of exercises of plantar flexion [46].

The second muscle activation mechanism consisted of performing different types of exercise, such as plantar flexion [3,15,16,19,24,26–28,34,37,45,46,48,50,52,54,55,60,64], leg extension [14,20,29,31,43,56,58,61,62], lumbar exercises [65,67,68], grip exercises [69], shoulder test [70,71], endurance exercise [36,57]. Some studies designed devices such as magnetic resonance-compatible ergometers, to perform activation exercises with the subject inside the scanner, and thus avoid the lag between the performance of the exercise and the acquisition.

There are two ways to organize the procedures: one option is to perform a first acquisition to determine the basal states, then to apply the activation protocol, and then to perform the acquisition to determine the functional changes in the muscles caused by the activation mechanism. The contrast obtained post-exercise vs. baseline status is found in

Table 1
Synthesis of studies in healthy subjects.

Reference	Population	Observed musculature	Activation protocol	Main results
BOLD				
Sanchez et al. 2010 [14]	10	Tibialis anterior muscle.	Leg extension and IHP	The BOLD measurement in muscle comes from the intravascular contribution alone, and the extravascular compartment has no significant influence.
Andreas (a) et al. 2011 [15]	14	Gastrocnemius muscles.	Plantar flexion and IHP	The combination of techniques allows characterizing the changes in vivo during ischemia and reperfusion mechanisms
Towse (a) et al. 2011 [16]	11	Tibialis anterior muscle.	Plantar flexion	The magnitude of post-contraction changes in blood saturation and changes in signal levels (BOLD) were reproduced by a one-compartmental vascular model.
Andreas (b) et al. 2012 [17]	12	Soleus, gastrocnemius and tibialis anterior muscles	IHP	BOLD allows to analyze the effect of the drug heme arginate.
Partovi (a) et al. 2012 [18]	8	Soleus and gastrocnemius muscles	IHP	The skeletal muscle BOLD effect depends largely on the strength of the magnetic field
Schewzow (a) et al. 2013 [19]	20	Soleus, gastrocnemius and tibialis anterior muscles	Plantar flexion and IHP	The proposed model allows estimating the HPV, MIV and TTP parameters automatically, providing greater robustness to the analysis
Larsen (a) et al. 2015 [20]	14	Tibialis anterior muscle	Contractions of the dorsiflexor muscles of the leg	BOLD allows to evaluate the micro-vascular reactivity to eccentric exercise.
Caterini et al. 2015 [56]	10	Vastus medialis muscles and biceps femoris	Quadriceps extensions	The presented model allows to analyze and quantify the BOLD response, before a quadriceps exercise.
Nishii (a) et al. 2015 [21]	16	Calf muscles set	IHP	The technique makes it possible to demonstrate significant differences in the parameters between smokers and non-smokers, indicating the presence of early deterioration of muscle blood flow response in smokers
Nishii (b) et al. 2015 [22]	6	Calf muscles set	IHP	The proposed model, based on multi-echo dynamic acquisitions, allows minimizing the effects of oxygenation, and thus reflects changes in blood volume.
Towse (b) et al. 2016 [23]	8	Gastrocnemius muscle	IHP	The BOLD response at 7T is up to 6 times greater than at 3T.
Towse (c) et al. 2016 [24]	13	Soleus muscle	Plantar flexion	The BOLD response to 7T reveals interindividual variability in the physiological responses to muscle contraction, in the magnitude of the BOLD signal, and in its temporal variations.
Stacy (a) et al. 2016 [25]	33	Soleus, gastrocnemius, tibialis anterior and peroneus muscles	IHP	The BOLD technique is feasible and capable of detecting regional differences in muscle tissue oxygenation between subjects with different levels of physical activity.
Stacy (b) et al. 2016 [63]	10	Foot muscles set	IHP	BOLD can provide useful information on functional improvements of therapeutic interventions.
Muller et al. 2016 [26]	6	Soleus, gastrocnemius and tibialis anterior muscles	Plantar flexion	A decrease in BOLD signal during plantar flexion was observed, the effect of which increases with the greater workload of exercise.
Tonson et al. 2017 [27]	25	Soleus and tibialis anterior muscles	Plantar flexion	BOLD allows associating a reduction in microvascular function in the leg muscles, independent of the level of physical activity.
Hurley et al. 2019 [28]	23	Soleus muscle	Plantar flexion	Through the BOLD acquisition, it is possible to demonstrate the improvement in aerobic capacity after a 12-week training program.
Larsen (b) et al. 2019 [29]	30	Tibialis anterior muscle	Leg extension and IHP	The technique allows to evaluate the role of oxidative stress and nitric oxide in the restoration of microvascular reactivity after eccentric exercise
Huang et al. 2020 [65]	50	Erector spinae muscles	Lumbar hyperextensions	BOLD and T2 mapping is an indirect, noninvasive assessment of lumbar supraspinatus muscle activity. It can provide deeper knowledge of muscle physiology.
ASL				
Decorte et al. 2014 [30]	8	Calf muscles set	IHP	Noninvasive techniques such as ASL allow the estimation of oxygen consumption.
Fulford et al. 2016 [31]	10	Rectus femoris muscle	Leg extension	ASL acquisition allows reliable measurements with low error levels.
Englund et al. 2016 [32]	50	Calf muscles set	IHP	pASL and pcASL are feasible to use to characterize hyperemia phenomena.
IVIM				
Karampinos et al. 2010 [33]	3	Soleus and gastrocnemio muscles	–	The study proposes an appropriate methodology to characterize the anisotropy of the capillary network in vivo, and to extract certain geometric parameters from the microvasculature of the calf muscle at rest.
Wurnig et al. 2015 [66]	13	Erector spinae muscles	–	The IVIM parameters depend on the choice of the threshold of *b* used in the adjustment
Filli et al. 2015 [69]	8	Superficial and deep flexor muscles, brachioradialis muscle, and extensor carpi radialis longus and brevis muscles.	Hand grip	The IVIM acquisition allows the simultaneous quantification of perfusion and diffusion at rest and after exercise
Nguyen (a) et al. 2016 [70]	6	SSc, SSp, IS, AD, LD and PD.	Lift- off test	IVIM is a feasible tool to investigate striated muscle perfusion, providing information on the selective increase in muscle blood flow.
Nguyen (b) et al. 2017 [71]	12	SSc, SSp, IS, AD, LD and PD.	Lift-off test and Jobe test	The selective increase in microvascular perfusion is evidenced after a specific muscle exercise of the shoulder, and suggests a

(*continued on next page*)

Table 1 (*continued*)

Reference	Population	Observed musculature	Activation protocol	Main results
				direct relationship between microvascular perfusion and duration of effort.
Mastropietro et al. 2018 [34]	12	Soleus and gastrocnemius muscles	Plantar flexion	The proposed sequence makes it possible to measure muscle perfusion during at least one simple exercise paradigm.
Yoon et al. 2018 [35]	95	Calf muscles set	-	Multiple quantitative parameters of multiparametric MRI imaging are sensitive to age-associated changes in the musculature.
Jungmann et al. 2019 [57]	8	Muscles of the gluteus and iliopsoas, thigh, leg and foot.	Walk and run	Specific activation patterns were demonstrated during walking and running activities.
Adelnia et al. 2019 [58]	8	Rectus femoris and adductor magnus muscles.	Leg extension	Different hyperemia trends were obtained in the younger and older subject groups, giving an interpretation of age-associated changes in microvascular function.
Ogura et al 2020 [36]	12	Calf muscles set	Up and down stairs	IVIM allows to analyze changes in capillary blood volume before and after exercise.
DCE				
Wright et al 2013 [52]	10	Calf muscles set	Plantar flexion	Simultaneous angiography and perfusion images were obtained to assess large and small vessels with a single contrast dose and to quantify perfusion.
Combined				
Elder et al. 2010 [59] *(ASL and BOLD)*	12	Dorsiflexor muscles	IHP	The empirical relationship between %HbO_2 and R_2* during arterial occlusion is demonstrated, and muscle perfusion was also quantified using ASL
Hiepe et al. 2014 [67] *(IVIM and BOLD)*	14	Lumbar muscles	Isometric back extension	The induced variations in the T_2* signal are related and associated with a change in muscle perfusion and intracellular metabolism.
Schewzow (b) et al. 2015 [37] *(ASL and BOLD)*	19	Soleus, gastrocnemius and tibialis anterior muscles	Plantar flexion	ASL provides a reliable quantification of perfusion at 7T and is able to identify post-exercise activated muscle groups.
Ohno et al. 2020 [64] *(IVIM and ASL)*	13	Tibialis anterior muscle	Plantar flexion	Plantar flexion exercise causes an increase in all IVIM parameters, in addition, a correlation between *D** and blood flow derived from ASL and *D* with T_2 was observed.

T_2*: *effective transverse relaxation time,* R_2*: (1/T_2*), HPV: *hyperemic peak value*, TTP: *time-to-peak,* NR: *no registry,* %HbO_2: *relative oxygen saturation of hemoglobin,* pcASL: *Pseudo-Continuous ASL,* pASL: *Pulsed ASL,* D*: *Pseudo-Diffusion*, D: *Diffusion coefficient,* IHP: *Ischemia-hyperemia paradigm,* SSp: *Supraspinatus;* SSc: *Subscapularis;* IS: *infrascapularis;* AD: *anterior deltoid;* LD: *lateral deltoid;* PD: *posterior deltoid.*

all IVIM images [33–36,51,57,58,61,64,66–71]. Another option is to perform continuous acquisitions to observe the dynamics of variation of the signal when applying the paradigm. This set-up is associated with the ischemia-hyperemia paradigm and the BOLD and ASL image.

3.2. BOLD imaging

Implementation. BOLD effect imaging was the most widely used among the three techniques of interest here: 22 published articles applied to healthy subjects and 11 to patients. The observation of the muscular BOLD response is quantified mainly through the following parameters, obtained from the analysis of transient changes in the hemodynamic curve. From the observed baseline level, used as a reference (100%), the minimum value reached during the induced ischemia phase is estimated, and it is called "Minimum Ischemia Value" (MIV). In the following re-oxygenation phase, the maximum value reached corresponds to the "Hyperemic Peak Value" (HPV), and according to Partovi et al. 2012 [18], it is considered the most relevant parameter as it reflects the metabolic rate of oxygen. The time required for the signal to reach the hyperemic peak after completion of cuff-induced ischemia is identified as the "time-to-peak" (TTP). To facilitate curve analysis, Schewzow et al. [19] proposed a model based on the sigmoid function plus the gamma variable to support the standardization of the evaluation of the parameters associated with BOLD in muscle.

Observation in healthy subjects. The observed values are summarized in Table 3. The heterogeneity in magnetic field strengths, studied muscles and activation schemes limits the possibility of estimating expected averaged values. Although Versluis et al. in 2011 observed a low reproducibility in BOLD as in Dynamic Contrast - Enhanced imaging (DCE), with a coefficient of variation (C.V.) of up to 51% in 10 patients with peripheral arterial disease at 1.5 T [38], several other studies highlight the reproducibility of BOLD observations: C.V. close to 10% and intraclass correlation of 0.95 are presented in [27]; Stacy et al reported good repeatability between visits [63]; and good reproducibility is reported between observers and between sessions at 3 T in 34 patients with critical limb ischemia [44]. Tonson et al. [27], in test–retest observations, show the stability of the BOLD measurements with coefficients of variation close to 10%, in 25 healthy subjects. Versluis et al. [38] also emphasize that TTP evaluation has good reproducibility both in healthy subjects and in patients and, therefore, it would be one of the interesting biomarkers of BOLD. The range of published values in healthy subjects is wide, which does not allow easy identification of convergence towards reference values. This variability could be related to the different activation paradigms used: the average HPV observed with the ischemia-hyperemia paradigm is 14.5% vs. 8.6% with the application of exercises. The same intrinsic or extrinsic physiological variation (nutritional, pharmacological, others) may also have influenced between subjects and sessions. Another aspect to consider is the influence of the magnitude of the magnetic field on the BOLD response: Partovi et al. [18] showed a response up to 10% greater between 1.5 T and 3 T, and Towse et al. [23], measured a variation of transverse relaxation times due to the BOLD effect up to 6 times greater between 3 T and 7 T.

The BOLD signal is related to oxygen consumption, blood volume, and the activation of muscle coupling mechanisms - oxygen consumption - vascular dynamics. In a quantitative analysis of the BOLD response in muscle, Towse et al. [16] emphasized that signal variation depends on the balance between O_2 delivery and consumption, which can be altered by physical activity. In this work, the peak of the BOLD signal could be predicted using a model based on the observed volume variation and the observed saturation change in Near InfraRed Spectroscopy (NIRS). The correlation coefficient between the variation of transverse relaxation time T2* and measurements of transcutaneous oxygen pressure ($TcPO_2$) has been estimated to 0.93 in healthy subjects and 0.90 in patients with systemic sclerosis [40], and with a high correlation coefficient between T2* and $TcPO_2$ in patients with PAD [51]. The variation in T2* also

Table 2
Summary of studies in subjects with pathology.

Reference	Population	Pathology	Observed musculature	Activation protocol	Main results
BOLD					
Slade et al. 2011 [60]	31	Patients with diabetes mellitus type I y II.	Dorsiflexor muscles	Plantar flexion	Patients with early diabetes do not present a significant alteration of the microvascular capacity when performing a brief muscle contraction exercise.
Partovi (b) et al. 2012 [39]	23	Patients with SSc	Soleus and gastrocnemius muscles	IHP	By comparing SSc patients with control subjects, BOLD is determined to be an appropriate method for identifying pathology-induced alterations.
Partovi (c) et al. 2013 [40]	24	Patients with SSc	Soleus and gastrocnemius muscles	IHP	In patients with SSc, BOLD has a good correlation with TcPO2-type measurements, evidencing the deficit in reoxygenation of the tissues of these types of patients
Ma et al. 2014 [41]	87	Pacientes con osteopenia and osteoporosis.	Soleus, gastrocnemius and tibialis anterior muscles	IHP	The BOLD response is significantly altered in patients with osteoporosis, indicating a reduction in the metabolic capacity of oxygen.
Partovi (d) et al. 2014 [42]	24	Patients with SSc.	Soleus and gastrocnemius muscles	IHP	BOLD presents an adequate correlation with the Laser Doppler Velocimetry technique, allowing to study the alterations caused in patients with SSc.
West et al. 2015 [43]	21	Patients with Turner syndrome (TS).	Vastus medialis muscle	Quadriceps extension	When comparing the microvascular function of patients with TS and control subjects, the technique allows us to observe that there is no significant alteration in these types of patients.
Bajwa et al. 2016 [44]	56	Patients with Critical Limb Ischemia (CLI)	Calf muscles set	IHP	In patients with CLI, BOLD allows detecting deficits in tissue perfusion, positioning itself as a tool with development potential.
Li et al. 2017 [45]	18	Patients with PAD.	Soleus, gastrocnemius and tibialis anterior muscles	Plantar flexion	BOLD, it is possible to observe different behaviors of the T2 * signal in patients with PAD, before a low intensity exercise.
ASL					
Pollak et al. 2012 [46]	35	Patients with PAD.	Soleus and tibialis anterior muscles	Plantar flexion	The pASL mode corresponds to a feasible technique for the quantification of blood flow before a plantar-type exercise, and allows differentiating patients with PAD from control subjects.
Grözinger et al. 2014 [47]	10	Patients with PAD.	Soleus and tibialis anterior muscles	IHP	pcASL allows the detection of changes in perfusion parameters in patients with PAD, before and after a Peripheral Transluminal Angioplasty (PTA)
Lopez et al. 2015 [48]	30	Patients with PAD.	Calf muscles set	Plantar flexion and IHP	The pASL acquisition, either with an activation by the ischemia-hyperemia paradigm or with a plantar flexion exercise, manages to quantify differences in patients with PAD, compared to healthy subjects.
Zheng et al. 2015 [62]	10	Patients with diabetes mellitus type I y II	Foot muscles set	Plantar flexion	It is possible to analyze alterations in regional perfusion in the feet of patients with diabetes
Chen et al. 2018 [49]	19	Patients with PAD presenting CLI.	Calf muscles set	IHP	The characterization of reactive hyperemia in patients with PAD reflects multiple aspects of the pathophysiology of the disease
IVIM					
Sigmund et al. 2019 [61]	49	Patients with dermatomyositis (DM)	Quadriceps, hamstrings and adductors	Leg stretch and contraction	The analysis of the diffusion metrics in patients with DM reveal spatial heterogeneities and differences in the diffusion and pseudo-diffusion parameters.
Federau et al. 2020 [68]	17	Patients with Adolescent idiopathic scoliosis (AIS)	Paraspinal muscles	Symmetrical back exercise	IVIM, manages to identify altered perfusion patterns in patients with AIS, compared to control subjects.
DCE					
Versluis et al. 2012 [53]	20	Patients with PAD	Calf muscles set	IHP	Using gadofosveset a reversible albumin binding contrast agent, estimation of the hyperemic fractional microvascular blood plasma volume is possible and reproducible. Volume was found significantly smaller in PAD patients.
Zhang et al. 2019 [3]	28	Patients with PAD	Calf muscles set	Plantar flexion	New indicators are proposed: muscle perfusion normalized by the whole body perfusion, as well as the ratio of gastrocnemius/soleus perfusion. No difference was found between elderly healthy and PAD in resting perfusion but patients showed substantially lower perfusion after exercises.
Conlin et al 2019 [54]	18	Patients with PAD	Calf muscles set	Plantar flexion	The arterial transit time is proposed as indicator of muscle function. ATT is lower in PAD patient than in age-matched healthy subjects, themselves with ATT lower than younger healthy subjects.
Li et al. 2019 [55]	16	Patients with PAD	Calf muscles set	Plantar flexion	A multistep method is proposed to support the identification of arterial input function, method based on spatial and temporal information from the MR images. Efficiency and accuracy are improved for perfusion quantification.
Combined					
Versluis et al. 2011 [38] (BOLD and DCE)	18	Patients with PAD.	Calf muscles set	IHP	Reproducibility of DCE and BOLD MRI was poor in patients with a CV up to 50.9%. The results of the DCE and BOLD MRI indicate that the perfusion responses in the calf muscles

(continued on next page)

Table 2 (*continued*)

Reference	Population	Pathology	Observed musculature	Activation protocol	Main results
					of patients with PAD were slower compared with healthy volunteers.
Wary et al. 2010 [50] (BOLD and ASL)	18	Patients with Glycogen Storage Disease Type III (GSD 3).	Soleus, gastrocnemius, tibialis anterior and peroneus muscles	Plantar flexion	The characterization of the GSD 3 disorder is improved through the acquisition of BOLD and ASL, allowing the quantification of independent indicators related to the disease.
Suo et al. 2018 [51] (IVIM, BOLD and ASL)	39	Patients with PAD	Soleus, gastrocnemius and tibialis anterior muscles	IHP	BOLD, IVIM and ASL, allow characterizing and obtaining complementary information on tissue perfusion in patients with PAD

PAD: *Peripheral Arterial Disease*, IHP: *Ischemia-hyperemia paradigm* SSc: *Systemic Sclerosis*, T2*: *Effective transverse relaxation time*, pASL: *Pulsed ASL*, pcASL: *Pseudo-Continuous ASL*.
Population reported corresponds to both patient and control subjects.

Table 3
Quantitative results of BOLD studies.

BOLD							
Reference	Healthy value Post-exercise			Pathology or specific condition	Value		
	HPV (%)	MIV (%)	TTP (s)		HPV (%)	MIV (%)	TTP (s)
Andreas (a) et al. 2011* [15]	24.0 ± 15.0	–	–	Con IPC	8 ± 13	–	–
Versluis et al. 2011* [38]	13.0 ± 5.9	–	60.7 ± 15.9	Patients with PAD	13.0 ± 6.4	–	116 ± 27
Towse (a) et al. 2011 [16]	3.4 ± 0.8	–	–	–	–	–	–
Slade et al. 2011 [60]	3.0 ± 0.5	–	–	Patients with T1D	2.0 ± 0.4	–	–
Slade et al. 2011 [60]	3.0 ± 0.5	–	–	Patients with T2D	1.0 ± 0.2	–	–
Andreas (b) et al. 2012* [17]	4.5 ± 0.6	–	221 ± 19	consumption of heme arginate	6.2 ± 0.6	–	175 ± 16
Partovi (a) et al. 2012* [18]	20.1 ± 11.0	−9 ± 3.5	33.5 ± 7.0	Patients with SSc	9 ± 13	−15.0 ± 7.3	39 ± 21
Partovi (b) et al. 2012* [42]	12.0 ± 6.0	−5.5 ± 2.8	42.8 ± 7.5	Acquisition with 3 T	21.6 ± 7.3	−7.8 ± 1.8	41 ± 9
Partovi (c) et al. 2013* [40]	22.2 ± 8.8	−8.9 ± 3.5	32.5 ± 8.7	Patients with SSc	7.9 ± 6.6	−14.7 ± 7.4	40.9 ± 14.5
Schewzow (a) et al. 2013* [19]	27.0 ± 24.0	–	168 ± 92	–	–	–	–
Ma et al. 2014* [41]	3.6 ± 5.0	−61.5 ± 17	–	Patients with osteoporosis	2.1 ± 9.7	−60.7 ± 12.0	–
Partovi (d) at al. [42] 2014*	22.2 ± 8.8	−8.9 ± 3.5		Patients with SSc	7.9 ± 6.6	−14.7 ± 7.4	
Nishii (a) et al. 2015* [21]	8 ± 2	–	45.4 ± 7.1	Smokers	8 ± 3	–	67.5 ± 18.8
Caterini et al. 2015 [56]	14 ± 6	–	9.6 ± 3.6	–	–	–	–
West et al. 2015 [43]	16 ± 8	–	9.4 ± 6.6	Patients with TS	13 ± 0.1	–	9.0 ± 4.6
Schewzow (b) et al. 2015 [37]	22 ± 10	–	161 ± 72	–	–	–	–
Bajwa et al. 2016* [44]	28 ± 14	−11.03 ± 5.6	68.7 ± 22.8	Patients with CLI	17 ± 11	−8.7 ± 5.1	64.5 ± 29.7
Stacy (b) et al. 2016* [63]	5.6 ± 1.6	−4 ± 2.8	75.9 ± 15.0	–	–	–	–
Muller et al. 2016 [26]	–	−2 ± 0.4	–	Triple Workload	–	−4.0 ± 0.7	–
Towse (c) et al. 2016 [24]	4.0 ± 0.6	–	9 ± 1	–	–	–	–
Tonson et al. 2017 [27]	5.0 ± 1.5	–	25 ± 4	Age condition	3.0 ± 0.6	–	27 ± 5
Larsen (b) et al. 2019 [29]	4.0 ± 3.0	–	12 ± 3	Antioxidant intake	4 ± 4	–	10 ± 4
Hurley et al. 2019 [28]	3.3 ± 1.0	–	32	Aerobic training	4.4 ± 1.4	–	25

HPV: *Hyperemic Peak Value*, TTP: *Time-To-Peak, MIV: Minimum Ischemia Value*, IPC: *ischemic preconditioning*, PAD: *Peripheral Arterial Disease*, T1D: *Type 1 diabetes*, T2D: *Type 2 diabetes*, HA: *heme arginate*, SSc: *Systemic sclerosis*, TS: *Turner syndrome*, CLI: *Critical Limb Ischemia*, *: *application of the "ischemia-hyperemia paradigm"*.
% values are presented with respect to initial baseline.

shows a high correlation with microperfusion changes estimated by laser Doppler flowmetry [42]. Based on data from NIRS, blood flow measured by ASL, and observation of the change in transverse relaxation times observed in BOLD, Elder et al. proposed a model to estimate the % HbO_2 consumed during muscle contractions [59]. Sanchez et al. showed that the observed effect is centered in the intravascular compartment, and the extravascular compartment is not responsible for the change in signal strength observed [14]. Using the understanding of this BOLD effect, another model has been proposed, based on the use of multiple echoes to minimize the blood oxygenation change effect to evaluate blood volume variation only [22].

After having initial observations that the BOLD effect effectively allowed the functional exploration of the muscle, several studies were generated to evaluate the impact of the response of the vasculature to different manipulations: the effect of smoking on vascular health was underlined, with a TTP of 33% longer in smoking subjects indicating a decreased muscle re-oxygenation capacity [21]; the effect of antioxidants on the musculature and its vasculature [29], or heme arginate on its protective effect against ischemic reperfusion injury [17] was also studied. The evaluation of training programs [20,28,65] and the effect of different levels of physical activity [25] has been successfully explored with BOLD imaging. In this direction, Hurley et al. [28] showed a 33% increase in the hyperemic peak value, and a 25% decrease in TTP in older adults with aerobic training compared to control subjects. The decrease in oxygen metabolic capacity was highlighted in older adults by Tonson et al. [27], where the hyperemic peak value was decreased by about 5% compared to young adults.

Observations in patients. Regarding the exploration of clinical applications, works are found in patients with vascular disease such as PAD or CLI [38,44,45,51], in systemic sclerosis [39,40,42], also in diabetes [60], in osteopenia and osteoporosis [41], in Turner syndrome [43] and in patients with glycogen storage disease type III [50]. The works on peripheral arterial disease show variation of parameters associated with the pathology: the time to peak is multiplied by almost 2 in patients with PAD, with no variation of hyperemic peak value in patients [38]. The dynamics of the weighted signal in T2 * during low-intensity exercises in patients is found significantly different in patients compared to healthy subjects, interpreted as the observation of the alteration of the hemodynamic stable state observed in healthy muscles during the exercises [45]. In patients with early type I and type II diabetes, no significant alteration was observed in the BOLD parameters, but yes in relation to age [60]. About systemic sclerosis, the ability of the technique to quantify the alteration in all parameters was evidenced, with a hyperemic peak value decreased by half or more compared to healthy subjects [39,40], and the slower TTP of 24% in patients [42]. BOLD imaging also shows an altered metabolic capacity for oxygenation in subjects with different levels of bone mineral density, observing how patients with osteoporosis and osteopenia present a decrease of close to 3% in HPV [41]. In this study, the different dynamics observed in the different muscle groups - soleus, gastrocnemius and tibialis anterior - have been associated with different vascular densities and endothelial function in them. Not showing significant differences in BOLD in patients with Turner Syndrome allowed West et al. to postulate that the poor tolerance of these patients to exercise is due rather to extravascular factors [43].

3.3. IVIM imaging

Implementation. There are fewer published studies that consider the use of the IVIM technique for muscle functional assessment in contrast to those based on BOLD: only 15 in the period studied, 3 of which in patients [51,61,68]. Several studies focused on highlighting the feasibility and interest of the technique in the functional study of different muscles [34,69–71]. Wurnig et al. [66], in their work, focused on a proposal to identify the threshold value of *b* for the IVIM in each organ, propose to consider the microperfusion portion for values of *b* lower than 150 s/mm^2 in the muscles. Regarding the implementation of the technique, in a similar way to that observed in the other organs, a variety of selected sets of *b* values is observed: with between 6 and 16 values of *b* used, with maximum *b* between 500 and 1000 s/mm^2.

Observation in healthy subjects. The IVIM technique proposes three parameters: *f*, micro-perfusion fraction, *D*, diffusion coefficient, and *D**, pseudo-diffusion coefficient. As shown in Table 4, the variation observed between studies in healthy subjects in the microperfusion fraction is ranging from 3.0 to 9.0% pre-exercise in healthy subjects, and up to 14% in patients. The interpretation of the increase observed after exercise has been proposed as a change of blood volume at the level of the microvasculature [36]. The diffusion coefficient, *D*, itself is also more stable, and consistent with the values commonly found in the literature [72,73]. This is consistent with the association of the diffusion coefficient to the microstructural parameters of the tissues, without varying in the context studied. The pseudo-diffusion coefficient, in turn, shows great variability between studies. This variability is similar to what is observed in works in other organs, where *D** is always shown as the most difficult parameter to estimate [11,74]. In this sense, Suo and colleagues also observed an ICC in muscle estimated to 0.77 for *f*, 0.92 for *D* and 0.64 for *D** [51]. Two papers combined the functional exploration techniques emphasizing the variation of BOLD and IVIM parameters associated with changes in muscle perfusion and intracellular metabolism [67] and underlining the correlation between D* and blood flow derived from ASL [64].

The IVIM allows to obtain maps of *f*, *D* and *D**, which allow detecting the muscular selectivity, that is, the differences in the increase of the parameters in certain muscles with the exercises performed: the antagonistic role of the subscapular/supraspinatus muscles with the infraspinatus could be observed when a shoulder test was performed [71]. Another study observed the muscle activation that involves going from a walk to a run, where the muscles most activated by the walk – quadriceps and gluteus – lower their activation parameters to give greater microvascular activity to the muscles of the lower leg and foot, which have a greater role in this exercise [57]. The relationship between age and vascular function was evaluated by two different groups, showing marked variation in *D** [35], or *f* [58].

Observations in patients. The use of IVIM in pathologies is scarce, finding three applications: in adolescent idiopathic scoliosis, where the alteration in perfusion patterns was evidenced before lumbar exercise, with difference in values close to 300% in *fD** in the concave zone vs. convex zone [68]. A decreased fraction of microperfusion was observed in patients with dermatomyositis, in contrast to healthy subjects, after a quadriceps exercise [61]. Finally, in patients with PAD, Suo et al. emphasized that the ASL, BOLD and IVIM provide complementary information regarding tissue perfusion, being in this study the BOLD signal the most reproducible and the only one to show differences between healthy subjects and patients [51].

3.4. ASL imaging

Implementation. As with IVIM, few ASL functional studies were identified: 6 in healthy subjects and 7 in patients. The attractiveness of the technique is that the interpretation of what is observed is more direct when estimating a commonly used parameter such as blood flow. Most studies used the pulsed mode of ASL (pASL) [30,31,37,46,48,49,62], rather than the pseudo-continuous mode (pcASL). An advantage with pASL is the best achievable temporal resolution, while pcASL allows better signal-to-noise ratio. Englund et al. stressed that both, pcASL and pASL, provide an accurate and consistent measurement of perfusion dynamics in reactive hyperemia [32].

Observation in healthy subjects. Several published studies focused on showing the feasibility of implementing the method to observe muscle function [30–32], even in high fields such as 7 T [37]. The post-

Table 4
Quantitative results of IVIM studies.

IVIM							
Reference	Values in healthy subjects or pre-exercise			Pathology or specific condition	Values in patients or post-exercise		
	f (%)	$D\left(\frac{mm^2}{s}x10^{-3}\right)$	$D^*\left(\frac{mm^2}{s}x10^{-3}\right)$		*f* (%)	$D\left(\frac{mm^2}{s}x10^{-3}\right)$	$D^*\left(\frac{mm^2}{s}x10^{-3}\right)$
Karampinos et al. 2010 [33]	3.76	1.74	18.6	–	–	–	
Hiepe et al. 2014 [67]	5.5 ± 3.2	1.69 ± 0.04	–	Back exercises	8.7 ± 2.5	1.73 ± 0.07	–
Wurning et al. 2015 [66]	7.4 ± 3	1.36 ± 0.04	21.7 ± 19	–	–	–	–
Filli et al. 2015 [69]	3 ± 1	1.45 ± 0.09	28.5 ± 11.4	Arm exercises	7 ± 3	1.68 ± 0.04	76 ± 59.1
Nguyen (a) et al. 2016 [70]	6.6 ± 1.6	1.46 ± 0.04	11.5 ± 3	Lift-off test	6.7 ± 1.8	1.48 ± 0.05	16.4 ± 4.5
Nguyen (b) et al. 2017 [71]	6.1 ± 1.7	1.49 ± 0.04	9.8 ± 1.5	Jobe test	7.8 ± 1.05	1.51 ± 0.04	20.2 ± 5.5
Mastropietro et al. 2018 [34]	6.8 ± 13	1.59 ± 3.8	33 ± 1.3	Plantar flexion	13 ± 6	1.72 ± 3.53	47.2 ± 2.23
Yoon et al. 2018 [35]	8.7 ± 1.6	1.6 ± 0.04	28 ± 4.8	Age condition	8.2 ± 1.57	1.5 ± 0.07	25.6 ± 4.06
Suo et al. 2018 [51]	5.6 ± 4.95	1.62 ± 1.61	19 ± 18.8	Patients with PAD	5.6 ± 9.45	1.51 ± 1.34	14.8 ± 13.6
Jungmann et al. 2019 [57]	5.7 ± 0.6	1.2 ± 0.18	10.9 ± 0.5	Muscle selectivity	7.6 ± 0.49	1.28 ± 0.2	12.7 ± 0.5
Adelnia et al. 2019 [58]	6.26 ± 0.9	2.43 ± 0.03	22.5 ± 2	Age condition	5.1 ± 0.98	2.35 ± 0.03	23.3 ± 2.28
Sigmund et al. 2019 [61]	9 ± 3.3	1.5 ± 0.15	39 ± 18.7	Patients with DM	8.7 ± 2.9	1.47 ± 0.16	31 ± 14.9
Federau et al. 2020 [68]	9 ± 5	1.4 ± 0.2	43 ± 51	Patients with AIS	14 ± 9	1.4 ± 0.4	37 ± 36
Ohno et al. [46] 2020 [64]	6.5 ± 3	1.55 ± 0.19	8.9 ± 4.8	Plantar flexion	13.1 ± 3.3	1.77 ± 0.12	20.6 ± 11.3

f: *perfusion fraction*, *D*: *diffusion coefficient*, *D**: *Pseudo-diffusion*, DM: *Dermatomyositis*, AIS: *Adolescent idiopathic scoliosis*.

exercise blood flow in healthy subjects presents a very wide range of published values (see table 5). This wide range can be due to the difference in the applied paradigms or intensity of the exercise in question, or even in the variability of the group called healthy. Similarly to what is observed in other functional techniques, the reproducibility obtained with the ischemia-hyperemia paradigm is better than with exercises: with ICC of 0.98 vs. 0.87 respectively [48].

Observation in patients. The main focus of applications has been on PAD to show the difference in flow in patients [46–49], or to quantify perfusion after percutaneous transluminal angioplasty [47]. In one study, PAD patients present an average value of blood flow after plantar flexion exercise decreased by about 40% compared to control subjects [46]. Similarly, patients with diabetes see their post-exercise blood flow value decreased, compared to healthy ones, by around 30% [62]. These observations suggest the ability of the technique to quantify the severity of pathologies and provide maps to study regional perfusion in regions of interest.

3.5. DCE

Implementation. A small number of studies using DCE in combination with exercising muscle has been found: only five during the last 10 years. Two of them used the ischemia-hyperemia paradigm, by Versluis et al. [38,53], the other three used different implementations of plantar flexions [3,54,55]. Even though the cuff inflation is a more externally controllable and reproducible paradigm, [38] seemed to indicate that DCE and BOLD reproducibility are low.

For the ischemia-hyperemia paradigm, cuff inflation was immediately followed by a single bolus of contrast agent, and followed by injection of saline bolus afterwards. For the exercise paradigm, contrast media was injected either five seconds before the end of the exercise [3,54,55], or 2 min after cessation of the exercise [52]. [3,54,55] injected 0.05 mmol/kg gadoteridol (ProHance, Bracco Diagnostics), while [52] used 0.1 mmol/kg Gd-DTPA (Magnevist; Bayer, Berlin, Germany) and [38] 15 mL of gadopentetate dimeglumine (Magnevist, Bayer HealthCare Pharmaceuticals, Berlin, Germany). Versluis et al [53] used 8 mL of gadofosveset (AblavarH, Lantheus Medical Imaging, Billerica, MA), a reversible albumin binding contrast agent that was shown to be used to evaluate the hyperemic fractional microvascular blood plasma volume. A simultaneous MRA and DCE acquisition was proposed by [52], using time-resolved MRA techniques to dynamically visualize arterial anatomy at different phases of contrast arrival.

Although there are different ways for perfusion quantification, the main idea is to determine AIF from signal in the arteries. This is sometimes a challenging task due to the vessels small sizes, especially in patients with vasculature alteration. Li et al [55] proposed a multistep method based on spatial and temporal information of the images to help the identification of the AIF and support the efficiency and accuracy of the analysis.

Observation in healthy subjects. All published studies underly that there were promising results that allowed to distinguish exercise-induced variation of perfusion in muscles, for instance going in average from 25 mL/100 g/min at rest to 48 mL/100 g/min after exercise [52]. Yet, few studies use the same parameters to quantify perfusion which limits comparison and synthesis. In addition to the variety of quantification, the protocols used to study the muscle functionality vary in intensity, which also makes the comparison between studies difficult. [3] observes perfusion after low-intensity exercise that can be in the same range as the ones reported by [52]: 36 ± 23 mL/100 g/min in the soleus; but after exhaustion exercise perfusion went up to 67 ± 31 mL/100 g/min. In this same work, the gastrocnemius perfusion in these two low-intensity and exhaustion exercise was reported to 107 ± 73 mL/100 g/min and 135 ± 53 mL/100 g/min respectively [3], emphasizing the muscle specificity in perfusion quantification.

To overcome difficulties intrinsic to comparison, Zhang et al. [3] proposed to use new parameters based either on ratio of perfusion between muscles – gastrocnemius to soleus in the calf case, permitting the observation of the different roles each muscle play in the walking sequence – or on a normalization to the whole body perfusion. This latter can be obtained from the same MR exam, by estimating cardiac output normalized then by body weight, with the cardiac output obtained through the Stewart-Hamilton equation [75]. The interest point in these new parameters is that their variation in a specific muscle would then indicate if its change in perfusion would come from heart rate variation or solely due to active hyperemia of this specific muscle. Zhang et al [3] showed the good repeatability of these parameters between different days, different workloads, different ages and in patient with PAD as well.

Observation in patients. Even though no difference in perfusion is shown in resting muscle between healthy subjects and PAD patients at matching age [3], patients show lower perfusion after exercising than subjects: in 43 ± 23 mL/100 g/min in gastrocnemius after low-intensity exercise vs. 107 ± 73 mL/100 g/min in healthy subjects, or 82 ± 61 mL/100 g/min vs. 135 ± 53 mL/100 g/min after exhaustion exercise. This emphasizes the need for the exploration of muscle functionality in addition to morphological studies or perfusion quantification in resting state. Similar results in PAD patients are found by Conlin et al [54] when quantifying arterial transit time: found lower in patient, 2.4 ± 1.2 s, than age-matched healthy subject, 3.2 ± 1.1 s, themselves lower than younger control, 4.3 ± 1.5 s. The difference in arterial transit time potentially challenges the implementation of ASL and the definition of post-labeling delays.

3.6. Multiple imaging techniques

Some of the included studies combined the techniques of interest here in different manners: either looking for relation between these techniques [38,51,64], or contrasting their results with other forms of functional exploration [50,59,67]. As ASL permits the measurement of a clearly understood parameter, it has been used to strengthen the interpretation of the IVIM parameters [64]. In this work, fD* is shown to correlate with blood flow before and after exercise, while the so-called "perfusion fraction" f does not. These results agree well with the review of the IVIM technique, where fD* is associated with blood flow,

Table 5
Quantitative results of ASL studies.

ASL			
Reference	Average value post-muscle activation blood flow		
	Value in healthy ml/min	Pathology or specific condition	Value ml/min
Wary et al. 2010 [50]	53 ± 9	Patients with GSD3	33 ± 12
Pollak et al. 2012 [46]	80 ± 23	Patients with PAD	48 ± 16
Grözinger et al. 2014* [47]	74 ± 52	Post-PTA	129 ± 80
Decorte et al. 2014* [30]	10.9 ± 4.2	–	–
Lopez et al. 2015* [48]	109 ± 39	Patients with PAD	34 ± 17
Zheng et al. 2015 [62]	104 ± 65	Patients with diabetes	73 ± 48
Schewzow (b) et al. 2015 [37]	27 ± 16	–	–
Englund et al. 2016* [32]	69 ± 28	Acquisition with pcASL	50 ± 26
Fulford et al. 2016 [31]	41.8 ± 11.1	High intensity exercise	49.5 ± 8.8
Chen et al. 2018* [49]	30.33 ± 5.82	Patients with CLI	28.42 ± 10.07
Ohno et al. 2020 [64]	38.9 ± 11.1	–	–

GSD3: *Glycogen Storage Disease type III*, PAD: *Peripheral Artery Disease*, PTA: *Percutaneous Transluminal Angioplasty*, pcASL: *Pseudo-Continuous ASL*, CLI: *Critical Limb Ischemia*.

* : Application of the "ischemia-hyperemia paradigm".

while f with blood volume and pseudo-diffusion D* with mean transit time [11]. Good agreement between ASL, BOLD and NIRS emphasized the possibility of estimating the relative oxygen saturation of hemoglobin during isometric contraction [59]. The relation between NIRS and BOLD signal is interesting as both relate with hemoglobin variation, in the venous circulation. Two papers combined IVIM or BOLD or ASL with magnetic resonance spectroscopy (MRS) of the ^{31}P to obtain additional insight on muscle physiology [50,67]. Changes induced by exercise in phosphocreatine, diffusion and perfusion were strongly associated with T2* increases, suggesting that T2* and perfusion sensitive sequences, as well as ^{31}P, permit to monitor muscle physiological changes during muscle fatigue [67]. Using BOLD, ASL and MRS of ^{31}P and ^{13}C to assess oxidative phosphorylation and glycogen quantitation, Wary et al [50] proposed that it is the alteration in perfusion that would be responsible for impaired post-exercise phosphocreatine recovery in patients with glycogen storage disease type III.

Few works focused on reproducibility, obtaining different conclusions. [38] emphasized the high C.V. of DCE and BOLD observation in PAD patients, of 51% in DCE and of 27% in BOLD, observed between scans separated by a few days. C.V. in healthy volunteers were found smaller (18% and 22% resp.). This raises the question on the stability of the perfusion-related variables in patients between sessions, as there could be intrinsic or extrinsic reasons for perfusion variations (circadian or hormonal or pharmacological variation, among others). On the other hand, the interscan reproducibility obtained in [51] was qualified as fair to excellent, with intraclass correlation coefficient ICC values ranging from and 0.55 for D* to 0.84 for D, with intermediate values of 0.67 for f, of 0.73 for blood flow, 0.85 for T2*. One of the difference in implementation between [51] and [38] is that the former worked at 3 T, and the latter at 1.5 T. Improved signal to noise ratio could explained the differences in reproducibility, but further studies are needed to reach a more robust conclusion. Suo et al. [51] is the only work that applied the three techniques, IVIM, ASL and BOLD, to the same cohort of healthy subjects and patients: even if all techniques show a response in cuff-induced ischemia in healthy subjects, only BOLD images managed to distinguish patients with PAD in all studied muscles, and to separate mild to severe PAD affectation. BOLD observations were independent of age in every muscle group, while ASL of all muscle groups and IVIM of the gastrocnemius group were influenced by age.

4. Discussion

It is necessary to emphasize in the first place the low number of subjects included in most of the studies: in applications in healthy subjects, the median number of persons was 12, with a median value of only 4.5 for women included. In patients, the median number of subjects included increases to 22, but these are still preliminary studies.

The 59 articles included in this review show the feasibility of implementing functional muscle exploration with MRI, in a varied range of muscles studied. They offer concrete set-up proposals for the activation of such or such muscle of interest. All techniques aim at the observation of hemodynamics, from different perspectives, either through the consumption of O2 and the variation of T2*, through the variation of the flow directly, or through the variation associated with perfusion and micro-perfusion.

The technique that has attracted the most attention of the community is BOLD imaging. No clear convergence towards reference values in healthy subjects is observed in the different studies, probably associated with the variability of ways used to stimulate muscles. The Time-To-Peak parameter seems to be the marker of greater stability for this type of imaging. One of the limitations may be that BOLD signal processing is not standardized in this context and has to be carried out manually, which may be susceptible to errors. The acquisition time is an aspect to be considered, especially in BOLD procedures or with continuous acquisition. While ASL has the advantage of being an easily interpretable technique - as it gives direct flow measurement - estimated values vary between studies. In case of wanting to implement BOLD or ASL studies in a new setting, it would be necessary to consider a control group to contrast the results with the patients with the protocol of choice. DCE also offers the advantage of being an easily interpretable technique as it aims at quantifying the tissue perfusion. Yet the few studies focused on exercise-driven perfusion variation use different ways of quantification and therefore limit a possibility of synthesis. The observations in IVIM show more convergence in their values. In the application in skeletal muscles, as what has been seen in other organs, the micro-perfusion fraction, *f*, seems to be the most stable marker to consider, associated with blood volume and its variation. It seems relevant to emphasize that IVIM and ASL offer the possibility of obtaining functional maps, while BOLD is more oriented to the quantification of the hemodynamic signal. Unlike its application in the brain, not much exploration has been seen of obtaining activation maps by fMRI in muscles.

5. Conclusions

A systematic review of the literature on the applications of four functional techniques by MRI of skeletal muscle was carried out in this work: BOLD, ASL, IVIM and DCE, over the last 10 years. The 59 selected studies show the feasibility of implementing this technique in various muscles and the utility of the estimated values in muscle health in different pathologies: in PAD, systemic sclerosis, diabetes, osteoporosis, adolescent idiopathic scoliosis and dermatomyositis, although the reference values in healthy subjects vary, probably in association with the stimulation paradigm used. Regarding clinical applications, the BOLD effect has been more widely studied compared to IVIM, ASL and DCE techniques. One of the actual challenges is to extend the validation of these initial studies to a greater number of subjects and towards a standardization of the observation method. To further extend these observations will allow a clearer perspective on the reproducibility of the quantitative measures offered here. These four techniques are based on sequences already present in conventional clinical MRI scanners, therefore, their use for the functional examination of muscles does not require additional investment in equipment. Having these non-invasive imaging tools, allowing the visualization and quantification of parameters associated with the vascular health of the muscles, can represent interesting support for musculoskeletal exploration beyond the actual routine morphological studies.

Declaration of Competing Interest

The authors declare that they have no known competing financial interests or personal relationships that could have appeared to influence the work reported in this paper.

Acknowledgement

SC acknowledges funding from ANID - FONIS grant #SA17I0124, from FONDEF IDeA ID20i10332, and support from Millennium Nucleus for Cardiovascular Magnetic Resonance, Chile.

References

[1] C. Castiglioni, J. Jofré, B. Suárez, Enfermedades neuromusculares, Epidemiología y Políticas de Salud en Chile, Rev Med Clin Condes 29 (6) (2018) 594–598.
[2] R. Valdebenito, Epidemiología de las enfermedades neuromusculares, Rehabil. Integral 10 (2) (2015) 62–63.
[3] J.L. Zhang, G. Layec, C. Hanrahan, C.C. Conlin, C. Hart, N. Hu, L. Khor, M. Mueller, V.S. Lee, Exercise-induced calf muscle hyperemia: quantitative mapping with low-dose dynamic contrast enhanced magnetic resonance imaging, Am. J. Physiol.-Heart Circul. Physiol. 316 (1) (2019) H201–H211.
[4] D. Le Bihan, E. Breton, D. Lallemand, M.L. Aubin, J. Vignaud, M. Laval-Jeantet, Separation of diffusion and perfusion in intravoxel incoherent motion MR imaging, Radiology 168 (2) (1988) 497–505.
[5] S. Ogawa, D.W. Tank, R. Menon, J.M. Ellermann, S.G. Kim, H. Merkle, K. Ugurbil, Intrinsic signal changes accompanying sensory stimulation: functional brain

mapping with magnetic resonance imaging, Proc. Natl. Acad. Sci. U S A 89 (13) (1992) 5951–5955.

[6] J.A. Detre, J.S. Leigh, D.S. Williams, A.P. Koretsky, Perfusion imaging, Magn. Reson. Med. 23 (1) (1992) 37–45.

[7] P.D. Gollnick, B. Sjödin, J. Karlsson, E. Jansson, B. Saltin, Human soleus muscle: a comparison of fiber composition and enzyme activities with other leg muscles, Pflugers Arch. 348 (3) (1974) 247–255.

[8] S.-G. Kim, Biophysics of BOLD fMRI investigated with animal models, J. Magn. Reson. 292 (2018) 82–89.

[9] C. Stippich, Preoperative blood oxygen level dependent (BOLD) functional magnetic resonance imaging (fMRI) of motor and somatosensory function, in: S. Ulmer, O. Jansen (Eds.), fMRI Basics and Clinical Applications, Springer, Berlin, 2010, pp. 51–68.

[10] M. Grade, J.A. Hernandez Tamames, F.B. Pizzini, E. Achten, X. Golay, M. Smits, A neuroradiologist's guide to arterial spin labeling MRI in clinical practice, Neuroradiology 57 (12) (2015) 1181–1202.

[11] C. Federau, Intravoxel incoherent motion MRI as a means to measure in vivo perfusion: A review of the evidence, NMR Biomed. 30 (11) (2017) e3780.

[12] D. Le Bihan, What can we see with IVIM MRI? Neuroimage 187 (2019) 56–67.

[13] P.S. Tofts, G. Brix, D.L. Buckley, J.L. Evelhoch, E. Henderson, M.V. Knopp, H. B. Larsson, T.Y. Lee, N.A. Mayr, G.J. Parker, R.E. Port, J. Taylor, R.M. Weisskoff, Estimating kinetic parameters from dynamic contrast-enhanced T(1)-weighted MRI of a diffusable tracer: standardized quantities and symbols, J. Magn. Reson. Imaging 10 (3) (1999) 223–232.

[14] O.A. Sanchez, E.A. Copenhaver, C.P. Elder, B.M. Damon, Absence of a Significant Extravascular Contribution to the Skeletal Muscle BOLD Effect at 3 T, Magn. Reson. Med. 64 (2) (2010) 527–535.

[15] M. Andreas, A.I. Schmid, M. Keilani, D. Doberer, J. Bartko, R. Crevenna, E. Moser, M. Wolzt, Effect of ischemic preconditioning in skeletal muscle measured by functional magnetic resonance imaging and spectroscopy: a randomized crossover trial, J. Cardiovasc. Magn. Reson. 13 (1) (2011), https://doi.org/10.1186/1532-429X-13-32.

[16] T.F. Towse, J.M. Slade, J.A. Ambrose, M.C. DeLano, R.A. Meyer, Quantitative analysis of the postcontractile blood-oxygenation-level-dependent (BOLD) effect in skeletal muscle, J. Appl. Physiol. 111 (1) (2011) 27–39.

[17] M. Andreas, A.I. Schmid, D. Doberer, K. Schewzow, S. Weisshaar, G. Heinze, M. Bilban, E. Moser, M. Wolzt, Heme arginate improves reperfusion patterns after ischemia: a randomized, placebo-controlled trial in healthy male subjects, J. Cardiovasc. Magn. Reson. 14 (2012).

[18] S. Partovi, A.-C. Schulte, B. Jacobi, M. Klarhöfer, A.B. Lumsden, M. Loebe, M. G. Davies, G.P. Noon, C. Karmonik, L. Zipp, G. Bongartz, D. Bilecen, Blood oxygenation level-dependent (BOLD) MRI of human skeletal muscle at 1.5 and 3 T, J. Magn. Reson. Imaging 35 (5) (2012) 1227–1232.

[19] K. Schewzow, M. Andreas, E. Moser, M. Wolzt, A.I. Schmid, Automatic Model-Based Analysis of Skeletal Muscle BOLD-MRI in Reactive Hyperemia, J. Magn. Reson. Imaging 38 (4) (2013) 963–969.

[20] R.G. Larsen, R.P. Hirata, A. Madzak, J.B. Frøkjær, T. Graven-Nielsen, Eccentric exercise slows in vivo microvascular reactivity during brief contractions in human skeletal muscle, J. Appl. Physiol. 119 (11) (2015) 1272–1281.

[21] T. Nishii, A.K. Kono, M. Nishio, K. Kyotani, K. Nishiyama, K. Sugimura, Dynamic Blood Oxygen Level-dependent MR Imaging of Muscle: Comparison of Postocclusive Reactive Hyperemia in Young Smokers and Nonsmokers, Magn. Reson. Med. Sci. 14 (4) (2015) 275–283.

[22] T. Nishii, A.K. Kono, M. Nishio, K. Kyotani, K. Nishiyama, K. Sugimura, Evaluation of blood volume by use of blood oxygen level-dependent magnetic resonance imaging in a cuff-compression model: usefulness of calculated echo time image, Japanese J. Radiol. 33 (7) (2015) 441–447.

[23] T.F. Towse, B.T. Childs, S.A. Sabin, E.C. Bush, C.P. Elder, B.M. Damon, Comparison of muscle BOLD responses to arterial occlusion at 3 and 7 Tesla, Magn. Reson. Med. 75 (3) (2016) 1333–1340.

[24] T.F. Towse, C.P. Elder, E.C. Bush, S.W. Klockenkemper, J.T. Bullock, R.D. Dortch, B.M. Damon, Post-contractile BOLD contrast in skeletal muscle at 7T reveals inter-individual heterogeneity in the physiological responses to muscle contraction, NMR Biomed. 29 (12) (2016) 1720–1728.

[25] M.R. Stacy, C.M. Caracciolo, M. Qiu, P. Pal, T. Varga, R.T. Constable, A.J. Sinusas, Comparison of regional skeletal muscle tissue oxygenation in college athletes and sedentary control subjects using quantitative BOLD MR imaging, Physiol. Reports 4 (16) (2016) e12903, https://doi.org/10.14814/phy2.12903.

[26] M.D. Muller, Z. Li, C.T. Sica, J.C. Luck, Z. Gao, C.A. Blaha, A.E. Cauffman, A. J. Ross, N.J.R. Winkler, M.D. Herr, K. Brandt, J. Wang, D.C. Gallagher, P. Karunanayaka, J. Vesek, U.A. Leuenberger, Q.X. Yang, L.I. Sinoway, Muscle oxygenation during dynamic plantar flexion exercise: combining BOLD MRI with traditional physiological measurements, Physiol. Reports 4 (20) (2016) e13004, https://doi.org/10.14814/phy2.13004.

[27] A. Tonson, K.E. Noble, R.A. Meyer, M.R. Rozman, K.T. Foley, J.M. Slade, Age Reduces Microvascular Function in the Leg Independent of Physical Activity, Med. Sci. Sports Exerc. 49 (8) (2017) 1623–1630.

[28] D.M. Hurley, E.R. Williams, J.M. Cross, B.R. Riedinger, R.A. Meyer, G.S. Abela, J. M. Slade, Aerobic Exercise Improves Microvascular Function in Older Adults, Med. Sci. Sports Exerc. 51 (4) (2019) 773–781.

[29] R.G. Larsen, J.M. Thomsen, R.P. Hirata, R. Steffensen, E.R. Poulsen, J.B. Frøkjær, T. Graven-Nielsen, Impaired microvascular reactivity after eccentric muscle contractions is not restored by acute ingestion of antioxidants or dietary nitrate, Physiol. Reports 7 (13) (2019), https://doi.org/10.14814/phy2.14162.

[30] N. Decorte, T. Buehler, E.C.D. Araujo, A. Vignaud, P.G. Carlier, Noninvasive Estimation of Oxygen Consumption in Human Calf Muscle through Combined NMR Measurements of ASL Perfusion and T-2 Oxymetry, J. Vasc. Res. 51 (5) (2014) 360–368.

[31] J. Fulford, A. Vanhatalo, Reliability of arterial spin labelling measurements of perfusion within the quadriceps during steady-state exercise, Eur. J. Sport Sci. 16 (1) (2016) 80–87.

[32] E.K. Englund, Z.B. Rodgers, M.C. Langham, E.R. Mohler, T.F. Floyd, F.W. Wehrli, Measurement of skeletal muscle perfusion dynamics with pseudo-continuous arterial spin labeling (pCASL): Assessment of relative labeling efficiency at rest and during hyperemia, and comparison to pulsed arterial spin labeling (PASL), J. Magn. Reson. Imaging 44 (4) (2016) 929–939.

[33] D.C. Karampinos, K.F. King, B.P. Sutton, J.G. Georgiadis, Intravoxel partially coherent motion technique: characterization of the anisotropy of skeletal muscle microvasculature, J. Magn. Reson. Imaging 31 (4) (2010) 942–953.

[34] A. Mastropietro, S. Porcelli, M. Cadioli, L. Rasica, E. Scalco, S. Gerevini, M. Marzorati, G. Rizzo, Triggered intravoxel incoherent motion MRI for the assessment of calf muscle perfusion during isometric intermittent exercise, NMR Biomed. 31 (6) (2018) e3922, https://doi.org/10.1002/nbm.v31.610.1002/nbm.3922.

[35] M.A. Yoon, S.-J. Hong, M.C. Ku, C.H. Kang, K.-S. Ahn, B.H. Kim, Multiparametric MR Imaging of Age-related Changes in Healthy Thigh Muscles, Radiology 287 (1) (2018) 235–246.

[36] A. Ogura, H. Sotome, A. Asai, A. Fuju, Evaluation of capillary blood volume in the lower limb muscles after exercise by intravoxel incoherent motion, Radiol. Med 125 (5) (2020) 474–480.

[37] K. Schewzow, G.B. Fiedler, M. Meyerspeer, S. Goluch, E. Laistler, M. Wolzt, E. Moser, A.I. Schmid, Dynamic ASL and T-2*-Weighted MRI in Exercising Calf Muscle at 7 T-A Feasibility Study, Magn. Reson. Med. 73 (3) (2015) 1190–1195.

[38] B. Versluis, W.H. Backes, M.G.A. van Eupen, K. Jaspers, P.J. Nelemans, E. V. Rouwet, J.A.W. Teijink, W.P.T.M. Mali, G.-W. Schurink, J.E. Wildberger, T. Leiner, Magnetic Resonance Imaging in Peripheral Arterial Disease Reproducibility of the Assessment of Morphological and Functional Vascular Status, Invest. Radiol. 46 (1) (2011) 11–24.

[39] S. Partovi, A.-C. Schulte, M. Aschwanden, D. Staub, D. Benz, S. Imfeld, B. Jacobi, P. Broz, K.A. Jäger, M. Takes, R.W. Huegli, D. Bilecen, U.A. Walker, Impaired skeletal muscle microcirculation in systemic sclerosis, Arthritis Res. Therapy 14 (5) (2012) R209, https://doi.org/10.1186/ar4047.

[40] S. Partovi, M. Aschwanden, B. Jacobi, A.-C. Schulte, U.A. Walker, D. Staub, S. Imfeld, P. Broz, D. Benz, L. Zipp, K.A. Jaeger, M. Takes, M.R. Robbin, R. W. Huegli, D. Bilecen, Correlation of Muscle BOLD MRI With Transcutaneous Oxygen Pressure for Assessing Microcirculation in Patients With Systemic Sclerosis, J. Magn. Reson. Imaging 38 (4) (2013) 845–851.

[41] H.T. Ma, J.F. Griffith, C. Ye, D.K. Yeung, X. Xing, P.C. Leung, J. Yuan, BOLD effect on calf muscle groups in elderly females with different bone mineral density, Annu. Int. Conf. IEEE Eng. Med. Biol. Soc. 2014 (2014) 5607–5610.

[42] S. Partovi, A.-C. Schulte, D. Staub, B. Jacobi, M. Aschwanden, U.A. Walker, S. Imfeld, P. Broz, D. Benz, L. Zipp, M. Takes, K.A. Jäger, R.W. Huegli, D. Bilecen, Correlation of skeletal muscle blood oxygenation level-dependent MRI and skin laser Doppler flowmetry in patients with systemic sclerosis, J. Magn. Reson. Imaging 40 (6) (2014) 1408–1413.

[43] S.L. West, C.S. O'Gorman, A.H. Elzibak, J. Caterini, M.D. Noseworthy, T. Rayner, J. Hamilton, G.D. Wells, Skeletal muscle microvascular function in girls with Turner syndrome, BBA Clin. 3 (2015) 25–30.

[44] A. Bajwa, R. Wesolowski, A. Patel, P. Saha, F. Ludwinski, M. Ikram, M. Albayati, A. Smith, E. Nagel, B. Modarai, Blood Oxygenation Level-Dependent CMR-Derived Measures in Critical Limb Ischemia and Changes With Revascularization, J. Am. Coll. Cardiol. 67 (4) (2016) 420–431.

[45] Z. Li, M.D. Muller, J. Wang, C.T. Sica, P. Karunanayaka, L.I. Sinoway, Q.X. Yang, Dynamic characteristics of T2*-weighted signal in calf muscles of peripheral artery disease during low-intensity exercise, J. Magn. Reson. Imaging 46 (1) (2017) 40–48.

[46] A.W. Pollak, C.H. Meyer, F.H. Epstein, R.S. Jiji, J.R. Hunter, J.M. DiMaria, J. M. Christopher, C.M. Kramer, Arterial Spin Labeling MR Imaging Reproducibly Measures Peak-Exercise Calf Muscle Perfusion A Study in Patients With Peripheral Arterial Disease and Healthy Volunteers, Jacc-Cardiovasc. Imaging 5 (12) (2012) 1224–1230.

[47] G. Grözinger, R. Pohmann, F. Schick, U. Grosse, R. Syha, K. Brechtel, K. Rittig, P. Martirosian, Perfusion Measurements of the Calf in Patients With Peripheral Arterial Occlusive Disease Before and After Percutaneous Transluminal Angioplasty Using MR Arterial Spin Labeling, J. Magn. Reson. Imaging 40 (4) (2014) 980–987.

[48] D. Lopez, A.W. Pollak, C.H. Meyer, F.H. Epstein, L.i. Zhao, A.J. Pesch, R. Jiji, J. R. Kay, J.M. DiMaria, J.M. Christopher, C.M. Kramer, Arterial spin labeling perfusion cardiovascular magnetic resonance of the calf in peripheral arterial disease: cuff occlusion hyperemia vs exercise, J. Cardiovasc. Magn. Reson. 17 (1) (2015), https://doi.org/10.1186/s12968-015-0128-y.

[49] H.J. Chen, T.L. Roy, G.A. Wright, Perfusion measures for symptom severity and differential outcome of revascularization in limb ischemia: Preliminary results with arterial spin labeling reactive hyperemia, J. Magn. Reson. Imaging 47 (6) (2018) 1578–1588.

[50] C. Wary, A. Nadaj-Pakleza, P. Laforêt, K.G. Claeys, R. Carlier, A. Monnet, S. Fleury, C. Baligand, B. Eymard, P. Labrune, P.G. Carlier, Investigating glycogenosis type III patients with multi-parametric functional NMR imaging and spectroscopy, Neuromuscul. Disord. 20 (8) (2010) 548–558.

[51] S. Suo, L. Zhang, H. Tang, Q. Ni, S. Li, H. Mao, X. Liu, S. He, J. Qu, Q. Lu, J. Xu, Evaluation of skeletal muscle microvascular perfusion of lower extremities by cardiovascular magnetic resonance arterial spin labeling, blood oxygenation level-

dependent, and intravoxel incoherent motion techniques, J. Cardiovasc. Magn. Reson. 20 (1) (2018), https://doi.org/10.1186/s12968-018-0441-3.
[52] K.L. Wright, N. Seiberlich, J.A. Jesberger, D.A. Nakamoto, R.F. Muzic, M. A. Griswold, V. Gulani, Simultaneous Magnetic Resonance Angiography and Perfusion (MRAP) Measurement: Initial Application in Lower Extremity Skeletal Muscle, J. Magn. Reson. Imaging 38 (5) (2013) 1237–1244.
[53] B. Versluis, M.H.G. Dremmen, P.J. Nelemans, J.E. Wildberger, G.W. Schurink, T. Leiner, W.H. Backes, Dynamic Contrast-Enhanced MRI Assessment of Hyperemic Fractional Microvascular Blood Plasma Volume in Peripheral Arterial Disease: Initial Findings, Plos One 7 (5) (2012).
[54] C.C. Conlin, G. Layec, C.J. Hanrahan, N. Hu, M.T. Mueller, V.S. Lee, J.L. Zhang, Exercise-stimulated arterial transit time in calf muscles measured by dynamic contrast-enhanced magnetic resonance imaging, Physiol. Reports 7 (1) (2019) e13978, https://doi.org/10.14814/phy2.13978.
[55] X.W. Li, C.C. Conlin, S.T. Decker, N. Hu, M. Mueller, L. Khor, C. Hanrahan, G. Layec, V.S. Lee, J.L. Zhang, Sampling arterial input function (AIF) from peripheral arteries: Comparison of a temporospatial-feature based method against conventional manual method, Magn. Reson. Imaging 57 (2019) 118–123.
[56] J.E. Caterini, A.H. Elzibak, E.J.S. Michel, B.W. McCrindle, A.N. Redington, S. Thompson, M.D. Noseworthy, G.D. Wells, Characterizing blood oxygen level-dependent (BOLD) response following in-magnet quadriceps exercise, Magn. Reson. Mater. Phys., Biol. Med. 28 (3) (2015) 271–278.
[57] P.M. Jungmann, C. Pfirrmann, C. Federau, Characterization of lower limb muscle activation patterns during walking and running with Intravoxel Incoherent Motion (IVIM) MR perfusion imaging, Magn. Reson. Imaging 63 (2019) 12–20.
[58] F. Adelnia, M. Shardell, C.M. Bergeron, K.W. Fishbein, R.G. Spencer, L. Ferrucci, D. A. Reiter, Diffusion-weighted MRI with intravoxel incoherent motion modeling for assessment of muscle perfusion in the thigh during post-exercise hyperemia in younger and older adults, NMR Biomed. 32 (5) (2019) e4072.
[59] C.P. Elder, R.N. Cook, M.A. Chance, E.A. Copenhaver, B.M. Damon, Image-Based Calculation of Perfusion and Oxyhemoglobin Saturation in Skeletal Muscle During Submaximal Isometric Contractions, Magn. Reson. Med. 64 (3) (2010) 852–861.
[60] J.M. Slade, T.F. Towse, V.V. Gossain, R.A. Meyer, Peripheral microvascular response to muscle contraction is unaltered by early diabetes but decreases with age, J. Appl. Physiol. 111 (5) (2011) 1361–1371.
[61] E.E. Sigmund, S.H. Baete, T. Luo, K. Patel, D. Wang, I. Rossi, A. Duarte, M. Bruno, D. Mossa, A. Femia, S. Ramachandran, D. Stoffel, J.S. Babb, A.G. Franks, J. Bencardino, MRI assessment of the thigh musculature in dermatomyositis and healthy subjects using diffusion tensor imaging, intravoxel incoherent motion and dynamic DTI, Eur. Radiol. 28 (12) (2018) 5304–5315.
[62] J. Zheng, M.K. Hastings, D. Muccigross, Z. Fan, F. Gao, J. Curci, C.F. Hildebolt, M. J. Mueller, Non-contrast MRI perfusion angiosome in diabetic feet, Eur. Radiol. 25 (1) (2015) 99–105.
[63] M.R. Stacy, M. Qiu, X. Papademetris, C.M. Caracciolo, R.T. Constable, A.J. Sinusas, Application of BOLD Magnetic Resonance Imaging for Evaluating Regional Volumetric Foot Tissue Oxygenation: A Feasibility Study in Healthy Volunteers, Eur. J. Vasc. Endovasc. Surg. 51 (5) (2016) 743–749.
[64] N. Ohno, T. Miyati, S. Fujihara, T. Gabata, S. Kobayashi, Biexponential analysis of intravoxel incoherent motion in calf muscle before and after exercise: Comparisons with arterial spin labeling perfusion and T-2, Magn. Reson. Imaging 72 (2020) 42–48.
[65] Y.-L. Huang, J.-L. Zhou, Y.-M. Jiang, Z.-G. Zhang, W. Zhao, D. Han, B.o. He, Assessment of lumbar paraspinal muscle activation using fMRI BOLD imaging and T2 mapping, Quantit. Imaging Med. Surgery 10 (1) (2020) 106–115.
[66] M.C. Wurnig, O.F. Donati, E. Ulbrich, L. Filli, D. Kenkel, H.C. Thoeny, A. Boss, Systematic analysis of the intravoxel incoherent motion threshold separating perfusion and diffusion effects: Proposal of a standardized algorithm, Magn. Reson. Med. 74 (5) (2015) 1414–1422.
[67] P. Hiepe, A. Gussew, R. Rzanny, C. Anders, M. Walther, H.C. Scholle, J. R. Reichenbach, Interrelations of muscle functional MRI, diffusion-weighted MRI and P-31-MRS in exercised lower back muscles, NMR Biomed. 27 (8) (2014) 958–970.
[68] C. Federau, D. Kroismayr, L. Dyer, M. Farshad, C. Pfirrmann, Demonstration of asymmetric muscle perfusion of the back after exercise in patients with adolescent idiopathic scoliosis demonstrated using intravoxel incoherent motion (IVIM) MRI, NMR Biomed. 33 (3) (2020).
[69] L. Filli, A. Boss, M.C. Wurnig, D. Kenkel, G. Andreisek, R. Guggenberger, Dynamic intravoxel incoherent motion imaging of skeletal muscle at rest and after exercise, NMR Biomed. 28 (2) (2015) 240–246.
[70] A. Nguyen, J.-B. Ledoux, P. Omoumi, F. Becce, J. Forget, C. Federau, Application of intravoxel incoherent motion perfusion imaging to shoulder muscles after a lift-off test of varying duration, NMR Biomed. 29 (1) (2016) 66–73.
[71] A. Nguyen, J.B. Ledoux, P. Omoumi, F. Becce, J. Forget, C. Federau, Selective microvascular muscle perfusion imaging in the shoulder with intravoxel incoherent motion (IVIM), Magn. Reson. Imaging 35 (2017) 91–97.
[72] M. Froeling, J. Oudeman, G.J. Strijkers, M. Maas, M.R. Drost, K. Nicolay, A. J. Nederveen, Muscle changes detected with diffusion-tensor imaging after long-distance running, Radiology 274 (2) (2015) 548–562.
[73] J. Oudeman, A.J. Nederveen, G.J. Strijkers, M. Maas, P.R. Luijten, M. Froeling, Techniques and applications of skeletal muscle diffusion tensor imaging: A review, J. Magn. Reson. Imaging 43 (4) (2016) 773–788.
[74] S. Chabert, J. Verdu, G. Huerta, C. Montalba, P. Cox, R. Riveros, S. Uribe, R. Salas, A. Veloz, Impact of b-Value Sampling Scheme on Brain IVIM Parameter Estimation in Healthy Subjects, Magn. Reson. Med. Sci. 19 (3) (2020) 216–226.
[75] J.L. Zhang, H. Rusinek, L. Bokacheva, Q. Chen, P. Storey, V.S. Lee, Use of cardiac output to improve measurement of input function in quantitative dynamic contrast-enhanced MRI, J. Magn. Reson. Imaging 30 (3) (2009) 656–665.